A COMPARISON OF LASER ULTRASONICS AND EMAT TEXTURE MEASUREMENTS IN ALUMINUM ALLOYS

W. Lu, S. Min, L. Peng, D. Hughes
Sandia National Laboratories
Livermore, CA 94551

BACKGROUND

Ultrasonic techniques, which measure elastic anisotropy, have been used to study texture and plastic anisotropy of sheet materials. Ultrasonic velocity measurements can determine the orientation distribution coefficients (ODCs) W_{400}, W_{420}, and W_{440} which are used to describe crystallographic orientation distributions [1]. For steel sheets, strong correlations have been observed between ultrasonic velocity and the formability parameters $\bar{r}$ and Δr [3]. The results for aluminum show a relationship between the ODC W_{440} and the degree of earing [2-3].

In addition to a metal sheet's formability and degree of earing, information about individual texture components is also needed in certain cases. A Goss component, for example, is necessary in the manufacturing of quality steel transformers but undesirable in plate forming and canning applications. Recent work suggests that W_{440} can indicate the presence of the cube texture verses deformation textures (brass, copper, S, etc.) [4]. Few studies are available, however, which attempt to distinguish between the various textures.

This paper presents some initial results on ultrasonic texture identification of aluminum sheets using the distinctive features captured within the slowness (or inverse velocity) curves. We begin with theoretical predictions of Lamb wave slowness curves of perfect textures (cube, Goss, brass) and compare them with measurements taken from two aluminum samples by an electromagnetic acoustic transducer (EMAT) system. A second set of measurements from a laser-based ultrasonic setup (for which theory has not yet been formulated) is then presented and discussed in the context of developing an on-line system used for texture screening.

Review of Progress in Quantitative Nondestructive Evaluation, Vol. 14
Edited by D.O. Thompson and D.E. Chimenti, Plenum Press, New York, 1995

THEORETICAL SLOWNESS CURVES

Consider a metal sheet with a cubic crystal structure. The stiffness matrix [c], normally given with respect to the crystal axes X-Y-Z, has the form

$$[c]=\begin{bmatrix} c_{11} & c_{12} & c_{12} & 0 & 0 & 0 \\ c_{12} & c_{11} & c_{12} & 0 & 0 & 0 \\ c_{12} & c_{12} & c_{11} & 0 & 0 & 0 \\ 0 & 0 & 0 & c_{44} & 0 & 0 \\ 0 & 0 & 0 & 0 & c_{44} & 0 \\ 0 & 0 & 0 & 0 & 0 & c_{44} \end{bmatrix} \tag{1}$$

For the convenience of engineering practice, the coordinate axes x-y-z are usually chosen to coincide with the rolling (RD), transverse (TD), and normal (ND) directions. If the sheet has a perfect texture $\{hkl\}\langle uvw\rangle$, then the base vectors of x-y-z are

$$\hat{i}=\frac{u\hat{I}+v\hat{J}+w\hat{K}}{\sqrt{u^2+v^2+w^2}} \text{ and } \hat{k}=\frac{h\hat{I}+k\hat{J}+l\hat{K}}{\sqrt{h^2+k^2+l^2}} \tag{2}$$

where $\hat{I}$, $\hat{J}$, and $\hat{K}$ are the base vectors of the X-Y-Z system. The stiffness matrix [c] will transform to the new coordinate system x-y-z according to

$$[c']=[\mathrm{M}][c][\mathrm{M}]^{\mathrm{T}} \tag{3}$$

where [M] is the transformation matrix. (Reference [5] contains details of the matrix transformation.) For waves propagating in the plane of the sheet x-y with the direction of propagation $\vec{\ell}=\ell_1\hat{i}+\ell_2\hat{j}$, the components of the generalized Christoffel Γ tensor are

$$\begin{aligned} \Gamma_{11} &= \tilde{c}_{11}\ell_1^2+2\tilde{c}_{16}\ell_1\ell_2+\tilde{c}_{66}\ell_2^2 \\ \Gamma_{12} &= \Gamma_{21}=\tilde{c}_{16}\ell_1^2+(\tilde{c}_{12}+\tilde{c}_{66})\ell_1\ell_2+\tilde{c}_{26}\ell_2^2 \\ \Gamma_{22} &= \tilde{c}_{66}\ell_1^2+2\tilde{c}_{26}\ell_1\ell_2+\tilde{c}_{22}\ell_2^2 \end{aligned} \tag{4}$$

where

$$\begin{aligned} \tilde{c}_{11} &= c'_{11}-c'^2_{13}/c'_{33}; & \tilde{c}_{66} &= c'_{66}-c'^2_{36}/c'_{33} \\ \tilde{c}_{22} &= c'_{22}-c'^2_{23}/c'_{33}; & \tilde{c}_{16} &= c'_{16}-c'_{13}c'_{36}/c'_{33} \\ \tilde{c}_{66} &= c'_{66}-c'^2_{36}/c'_{33}; & \tilde{c}_{26} &= c'_{26}-c'_{23}c'_{36}/c'_{33} \end{aligned}$$

are the components of the modified stiffness matrix for a thin plate [6]. The eigenvalues of Γ correspond to ρv^2, where ρ is the density of the material and v is the phase velocity. One of the eigenvectors, which indicates the direction of particle motion, is equal (or close) to the direction of propagation. The corresponding velocity is that of the Lamb wave.

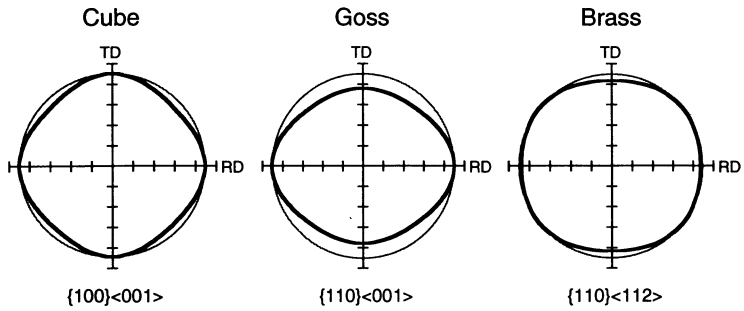

Figure 1: Theoretical slowness curves for cube, Goss, and brass textures.

Figure 1 shows the calculated theoretical Lamb wave slowness curves of cube {100}<001>, Goss {110}<001>, and brass {110} <112> textures. The drawing is normalized to the maximum velocity inverse and exaggerated. In each case, the slowness curve and a reference unit circle are shown. Note that the origin corresponds to a value of 0.5. Clearly, each texture has a distinctive slowness curve. For the cube texture, symmetry is preserved across each quadrant with maximum and minimum velocities occurring at ±45° and 0° with respect to the RD, respectively. In contrast, the maximum velocity for the Goss texture is along the TD. Although not as strong, the velocities for the brass texture have the opposite tendencies compared to that of the cube, having a minimum velocity at approximately ±45° and a maximum velocity along the TD.

Experimentally derived r-values can also be theoretically calculated based on texture information and a deformation model. Ren [7] evaluated and demonstrated the effect of individual texture components on r-values using the Taylor/Bishop and Hill (TBH) theory. The results show that a brass component has low r-values along the RD and TD and higher r-values in between. For a cube texture, the r-values are high along both the RD and TD, but low at ±45°. The Goss texture has a high r-value along the TD but remains low from the RD to ±45°.

EXPERIMENTAL METHOD

Test Material

Two AA2034-T4 aluminum plates 1/32" in thickness, provided by the Reynolds Metals Company, were used for this study. Table 1 lists the measured r-values for each sample along the RD, 45°, and TD. From Ren's results the high r(TD) relative to r(RD) for sample A indicates the presence of a Goss component whereas sample B is considerably more isotropic in the plane of the sheet. The slight increase in r-value at 45° suggests that sample B contains some rolling deformation texture components.

EMAT Results

Velocity versus angle measurements were obtained from a Lamb wave EMAT set which included a transmitter and two receivers separated by a fixed distance of 60 mm. The

Table 1: Measured r-values for two AA2034-T4 aluminum plates provided by Reynolds Metals Co. Plate thickness is 1/32".

	A	B
r (RD)	0.593	0.599
r (45°)	0.650	0.729
r (TD)	1.107	0.678

fundamental mode Lamb wave S_0 was generated by the transmitter and had a wavelength of about 12 mm. The measured slowness curves for samples A and B are shown in Figure 2. Again, the drawings are normalized to the maximum velocity inverse and plotted with a reference unit circle. Although the exaggeration scale has been increased by more than an order of magnitude with the center now being equal to 0.97, the features previously mentioned for the Goss texture, namely the maximum and minimum velocities at the TD and RD, respectively, are apparent in sample A. As expected, sample B is more isotropic with a velocity minimum near 45°. This indicates the presence of a deformation texture.

Optical Measurements

An optical system, consisting of a pulsed generation laser operating at a wavelength of 1064 nm, a continuous wave (CW) illumination laser operating at 532 nm, and a confocal Fabry-Perot interferometer sensitive to a combination of surface displacements and velocities, was used for ultrasonic excitation and detection in the arrangement shown in Figure 3. Unprepared samples were mounted on a rotational stage and beam paths were kept fixed for each set of measurements. Figure 4 is a typical single shot and 50-shot averaged interferometer signal for a 1/32" aluminum plate. Time-of-flight (TOF) information was extracted from this signal by applying a correlation algorithm with a reference waveform over a given window of the data set. Subsequent curve-fitting improved the resolution to less than the sampling interval of 5 ns.

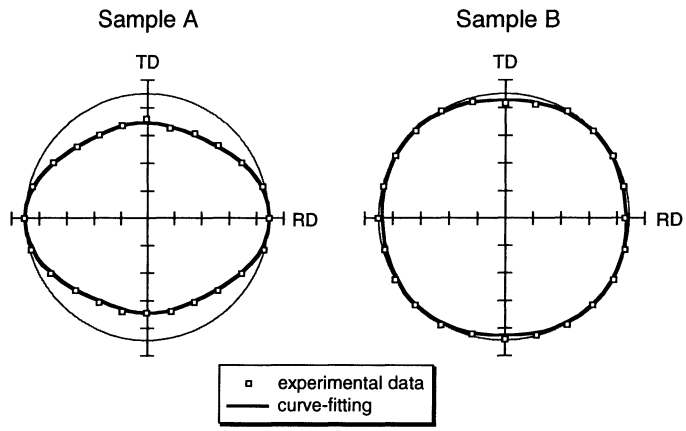

Figure 2: Experimental EMAT results for samples A and B.

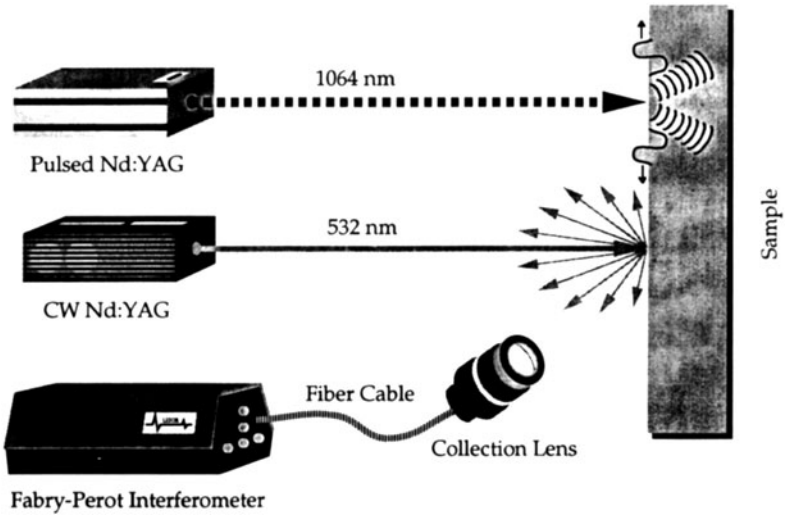

Figure 3: Schematic of LU setup. The test sample is mounted on a rotational stage.

It was observed that small differences in sample orientation caused significant variations in the computed TOF. Unlike EMATs which require propagation lengths of several inches due simply to the size of each tranducer, LU's point generation and detection allows the source and receiver to be placed a few millimeters apart, if desired. Texture effects previously on the order of several tens of nanoseconds are thus scaled down to a few nanoseconds. Consequently a slight misorientation from one measurement to the next causing a propagation length change of a few tens of microns will easily mask any texture-dependent velocity variations.

This phenomenon occurs when the sample surface is not perpendicular to the axis of rotation. In this case, the measured path length does not remain constant as assumed but varies as a function of the rotation angle θ. A mathematical description which allows us to predict, as well as an algorithm to correct for, this path length change has been formulated and will be presented in another article. Numerical calculations were performed to determine the range of θ over which this correction algorithm holds. Using actual direction vectors and lengths obtained from our experimental setup and an upper limit of ± 15 μm (corresponding to a Rayleigh wave travel time of 10 ns in aluminum) for the path length change, we determined the maximum allowable tilt without correction to be 0.1 degrees. In contrast post-processing affords us a 3.5 degree range of tolerable misalignment.

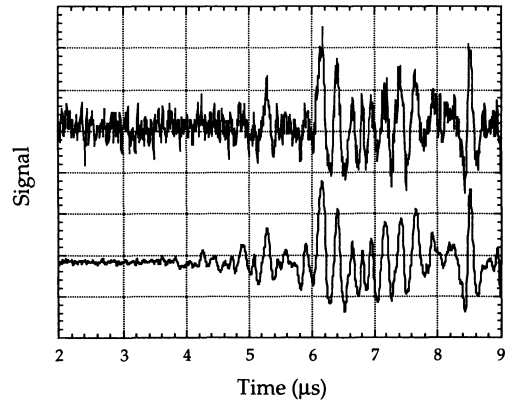

Figure 4: Typical single shot (top trace) and 50-shot averaged (bottom trace) interferometer signal.

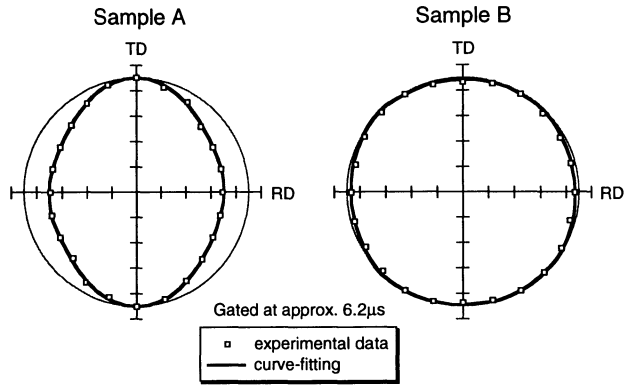

(a)

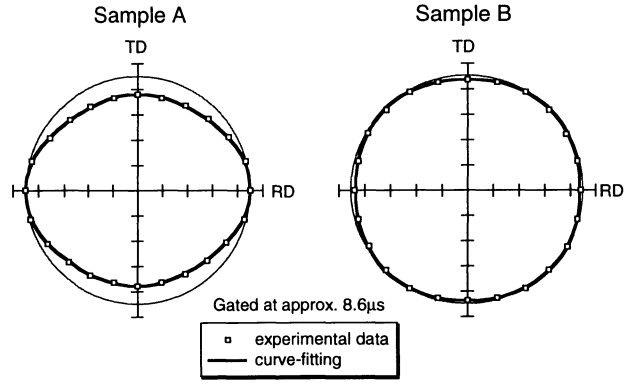

(b)

Figure 5: Experimental LU slowness curves. (a) Data window taken at 6.2 μs. (b) Data window at 8.6 μs.

Figure 5 shows the processed slowness curves for samples A and B obtained from optical measurements. The exaggeration scale has been kept the same as in figure 2. It is important to note that figures 5(a) and 5(b) differ only in the data window selected for TOF processing. In both cases, the basic trends for Goss texture, namely the velocity difference between the RD and TD, are again apparent in sample A while sample B is noticeably more isotropic.

DISCUSSION

As discussed earlier, theoretical Lamb wave slowness curves carry distinct features of individual texture components. We have shown that experimentally measured slowness curves of S_0, taken by an EMAT system, closely resemble the predicted curves and correctly reveal the major texture component of each sample. The slowness curves obtained from LU measurements also exhibit similar characteristics. Since a point laser source generates mixed mode waves, however, the acquired waveforms (fig. 4), and hence

results, are more difficult to interpret analytically. Figure 5 shows that by selecting various waveform peaks, slowness curves displaying the same basic trends but oriented differently are obtained. This is expected since the effect of texture on each mode, or combination of modes, is different. To gain a better understanding of these results, a model which can predict LU waveforms is needed in order to identify the mode of the wave from which the measurements are taken. Development of this theoretical foundation is now in progress.

Nonetheless, these results demonstrate the feasibility of using optical ultrasonic techniques for on-line texture determination. Even when operating in single shot mode, processed LU TOFs experience no degradation in accuracy. For engineering applications, LU slowness curves can simply be calibrated against EMAT measurements which have been shown to match the theoretical model. These results also show the potential of evaluating texture quantitatively from a slowness curve. A theoretical description, however, is still needed to obtain more percise texture information.

ACKNOWLEDGEMENTS

The aluminum samples were supplied by the Reynolds Metals Company. We thank Dr. Armand J. Beaudoin, Jr. for providing materials and technical information. This work is supported by the U. S. Department of Energy under contract# DE-AC04-94AL85000 and is part of the Sandia Lab-Directed Research and Development (LDRD) program.

REFERENCES

1. R. B. Thompson, J. F. Smith, S. S. Lee, and G. C. Johnson, Metall Trans 20, 2431 (1989).
2. R. B. Thompson, E. P. Papadakis, D. D. Bluhm, G. A. Alers, K. Forouraghi, H. D. Skank, and S. J. Wormley, J. NDE 12, 45 (1993).
3. W. Y. Lu, J. G. Morris, and Q. Gu, in Review of Progress in QNDE, Vol. 10, eds. D. O. Thompson and D. E. Chimenti (Plenum, New York, 1991), p. 1983.
4. B. Ren, J. G. Morris, and W. Y. Lu, Alumitech '94.
5. B. A. Auld, Acoustic Field and Waves in Solids, (Robert E. Krieger Publishing Company, Florida, 1990).
6. W. Tang, "Ultrasonic Measurements of Residual Stresses in a Thin Plate", MS Thesis, University of Kentucky, 1990.
7. B. Ren, "Studies of Rolling Texture and Microstructure Evolution as well as Plastic Anisotropy of Al-Mg Alloys", Ph.D. Dissertation, University of Kentucky, 1994.